Evaluation of the Surface Free Energy of Spin-Coated Photodefinable Epoxy

MARKUS P. K. TURUNEN, TOMI LAURILA, JORMA K. KIVILAHTI

Laboratory of Electronics Production Technology, Department of Electrical and Communications Engineering, Helsinki University of Technology, P.O. Box 3000, HUT FIN-02015, Finland

Received 8 March 2002; revised 13 June 2002; accepted 26 June 2002
Published online 7 August 2002 in Wiley InterScience (www.interscience.wiley.com). DOI: 10.1002/polb.10274

ABSTRACT: The surface free energy of crosslinked photodefinable epoxy (PDE) was evaluated from the advancing contact angles measured by the sessile drop method. Poly(tetrafluoroethylene) (PTFE) was used as a reference material in the evaluation of the surface free energies by various models. Pure water, diiodomethane, formamide, ethylene glycol, diethylene glycol, glycerol, 1-bromonaphthalene, decane, and tetradecane were used as the probing liquids. The surface free energies for PDE and PTFE were calculated to be 43.6 and 21.2 mJ/m^2, respectively. The contact-angle measurements indicated the isotropy of the PDE surface with respect to the surface free energy. The PDE coating was further characterized with scanning electron microscopy and atomic force microscopy. The PDE surface was treated chemically and by reactive ion etching (RIE) to determine their impact on the wettability and adhesion. The treatments resulted in decreased contact angles between the crosslinked PDE surface and water as the polarity of the surface increased from about 9% to 18 and 43% by the chemical and RIE treatments, respectively. On the contrary, the surface free energy of the treated PDEs, as calculated by the geometric mean model, did not change markedly (to 47.4 and 41.8 mJ/m^2 by the chemical and RIE treatments, respectively). Consequently, the contact angles of diiodomethane and the PDE solution on the treated surfaces did not decrease noticeably. The stud-pull test showed improved adhesion strength for PDE that was left less crosslinked and, therefore, had residual affinity against the sequential PDE layer. J Polym Sci Part B: Polym Phys 40: 2137–2149, 2002
Keywords: photoresists; sessile drop; printed wiring board; adhesion; surfaces

INTRODUCTION

In many applications, the performance of a polymer product is related to its surface properties. An example is a multilayer printed wiring board (PWB), in which dissimilar materials, including various polymers, are sequentially built up to enable high-density interconnection substrates.[1–10] For adequate adhesion between the layers, the surface free energy of a solid polymer has to be high enough to ensure proper wettability.[11,12] However, the topmost layer should prevent the adherence of dust and other contaminants. Moreover, it should serve as a diffusion barrier against liquids [especially water (H_2O)] and gases. Overall, the manipulation of the surface free energy at various interfaces during the sequential build-up process is essential for the reliable fabrication of PWBs.

The evaluation of the surface free energy has been used to predict adhesion and wettability.[13] Although the direct measurement of the surface free energy of a solid is impossible, indirect meth-

Correspondence to: J. K. Kivilahti (E-mail: jorma.kivilahti@hut.fi)

Journal of Polymer Science: Part B: Polymer Physics, Vol. 40, 2137–2149 (2002)

ods to evaluate the surface free energies of polymers have been developed.[14] The measurement of sessile drop contact angles of appropriate probing liquids with a known surface tension on a given solid surface provides a feasible method of obtaining the solid surface free energy value (γ_s). Incisive criticism against the method has been presented.[15] However, even those authors admitted, in their extensive re-evaluation of the data measured by the conventional goniometer technique, that properly executed measurements could be used to evaluate the surface free energy of solids.[16] There are several models in the literature for determining γ_s from the contact angles. These models have been thoroughly covered, and their differences are discussed elsewhere.[12,17–26] A brief review of the models is given later.

The well-known Young's equation is the basis of all the models used to determine the surface free energy here. Young's equation interrelates the equilibrium contact angle (θ) at the three-phase contact line and the interfacial surface free energies at the solid–vapor (γ_{sv}), liquid–vapor (γ_{lv}), and solid–liquid (γ_{sl}) interfaces. The required assumptions are that the liquid drop rests on an ideally smooth, chemically homogeneous solid surface that is not affected (swollen or partially diluted) by the liquid. In addition, the molecular chain orientation of the solid polymer[27] and adsorption layers on the surface may also affect the measured contact angle. However, for hydrophobic low-energy solid surfaces, there is only a small difference in the observed contact angles (less than the detection limit of the goniometer) measured in air or under vacuum for high-boiling-point liquids.[28] This leads to the approximation $\gamma_{sv} \approx \gamma_s$, in which the spreading pressure (π_e) is considered to be negligible.[28,29]

Previously, filled photodefinable epoxies (PDEs) have been used in the preparation of sequentially built-up integrated modules.[30] Chemical roughening of the filled epoxies has enabled good adhesion between the built-up layers.[11,31] Unfortunately, a rough surface leads to deteriorated electrical characteristics in high-frequency applications.[32] For smoother interfaces and more precisely defined structures, unfilled epoxies have to be employed. Unfilled PDEs lack good adhesion properties, and their roughening for mechanical anchoring is difficult.[33] The use of alternative treatments to improve adhesion has to be considered for minimizing the difficulties related to the mechanical, thermal, and environmental stability of highly miniaturized electronic assemblies. Therefore, the surface properties have to be studied in more detail to control adhesion and wettability. To the best of our knowledge, no extensive study of the surface free energies of PDEs applicable to electronics manufacturing has been published previously.

Therefore, the objective of this study was to evaluate the surface free energy from the contact-angle measurements performed for commercial solid PDE. Because of discrepancies between the models generally used in the determination of the surface free energy, an evaluation of some of the models was performed to obtain reliable information about the PDE surface. The surface was also modified by chemical and reactive ion etching (RIE) treatments, and their impact on the wettability and adhesion properties is discussed.

MATERIALS AND METHODS

Materials

The studied polymers were the commercially available PDE resin Epon SU-8 (Shell Chemical) and poly(tetrafluoroethylene) (PTFE; Goodfellow, Ltd.), which was used as a reference material. The PDE solution was composed of the epoxy resin (50.7 wt %), a γ-butyrolactone solvent (46.8 wt %), and a photoinitiator (2.5 wt %). The photoinitiator was triarylsulfonium hexafluoroantimonate salt provided as a 50:50 (w/w) mixture in polypropylene carbonate. The photoinitiator was purchased from Aldrich. The number-average molecular weight of the PDE resin was 7000 g/mol according to the manufacturer. PTFE was used (as received as a 0.5-mm-thick film) as a reference material in the contact-angle measurements. A glass-fiber-reinforced epoxy PWB substrate (FR-4) was purchased from PIAD Spa. The polymers were properly purified before the measurement of the contact angles.

The following were chosen as the probing liquids for the contact-angle measurements: H_2O (distilled), diiodomethane (DIM; Fluka), formamide (FA; J.T. Baker), ethylene glycol (EG; Aldrich), diethylene glycol (DEG; Aldrich), 1-bromonaphthalene (1-Br; Aldrich), glycerol (GL; Fluka), decane (DEC; Fluka), and tetradecane (TET; Fluka). The liquids were high-purity-grade and were used as received. The generally accepted surface tension parameters for the probing liquids are listed in Table 1.[17,34,35]

Table 1. Surface Tension Parameters (mN/m) of the Probing Liquids[17,34,35]

	γ_{Iv}	γ_{Iv}^{d}	γ_{Iv}^{p}	γ_{Iv}^{AB}	γ_{Iv}^{LW}	γ_{Iv}^{+}	γ_{Iv}^{-}
H_2O	72.8	21.8	51.0	51.0	21.8	25.5	25.5
DIM	50.8	48.5	2.3	0	50.8	0	0
FA	58.2	39.5	18.7	19.0	39.0	2.28	39.6
GL	63.4	37.0	26.4	30.0	34.0	3.92	57.4
1-Br	44.6	32.8	11.8	0	44.4	0	0
EG	48.2	29.0	19.2	19.0	29.0	1.92	47.0
DEG	44.4	31.7	12.7	—	—	—	—
DEC	23.8	23.8	0	0	23.8	0	0
TET	26.7	26.7	0	0	26.6	0	0

Cuprolite PHP92 swelling (18 vol % EG and 1.5 wt % NaOH in H_2O), Epoxymod MLX60 etching (4 wt % $KMnO_4$ and 1.5 wt % NaOH in H_2O), and neutralizing solutions (3.5 vol % H_2SO_4 and 0.7 vol % H_2O_2 in H_2O) were prepared from the master batches according to the supplier's (Alfachimici) recipe.

Bison polyurethane adhesive was used to attach the studied coatings to the stud of the adhesion testing equipment.

Procedure for Preparing the PDE Thin Films

The PDE solution was spin-coated on the PWB substrate (5 cm × 5 cm) at the speed of 1500 rpm for 10 s. After the coating, the samples were prebaked at 90 °C for 30 min to remove the solvent and were then exposed to ultraviolet light (365 nm, 17 mW/cm^2) for 40 s. The two-step crosslinking bake process was 30 min at 90 °C and 60 min at 140 °C in a flowing-air oven. The preparation of the coatings was carried out in a clean room to avoid surface contamination.

The prepared coating surfaces were treated with wet chemical and RIE treatments. The three-step chemical treatment was started by the exposure of the specimens to the swelling solution for 1 min at 75 °C. This was followed by the etching solution for 5, 10, 15, and 20 min at 70 °C. Finally, the surfaces were neutralized for 1 min at room temperature to remove the adsorbed MnO_2 from the surface. In the RIE system, the plasma was produced in the region between two electrodes, and the sample was placed directly below the plasma on a plate shielding the lower electrode. This was powered by a 13.56-MHz radio-frequency generator. The surface modification was performed with a O_2/CF_4 (15/5 sccm) gas mixture. The radio frequency (RF) power was 80 W, and the process pressure was held in the range of 20–50 mTorr. The treatment times were 5, 10, 15, and 20 min. Cleaning with ethanol followed the treatments.

Characterization

The sessile drop method with an Advanced Surface Technology goniometer equipped with a VCA 2500XE video contact-angle system was employed in the contact-angle measurements. A liquid drop (0.1 μL) was deposited on a solid polymer substrate with a microsyringe, and the advancing contact angle was measured. The measurements were conducted in air (21 ± 1 °C and 50 ± 3% relative humidity). The contact angles presented for each system were averages of eight drops placed on a given substrate.

A scanning electron microscope (JEOL 6335F/Oxford INCA) was used to examine the cross-sectional fracture surface of the coating. The polymer specimen was frozen in liquid nitrogen, and a sharp bending force was applied manually to break the coated substrate. The specimen was sputter-deposited with gold for examination in the scanning electron microscope. The acceleration voltage used during the investigations was 5 kV.

The topology of the PDE surface was studied with a Digital Instrument D3100 atomic force microscope. An area of 10 μm × 10 μm was scanned with silicon tips in the tapping mode. The arithmetic mean of the surface roughness (R_a) was calculated from the roughness profile determined by atomic force microscopy (AFM).

Fourier transform infrared (FTIR) spectroscopy was performed with a Nicolet Magna FTIR 750 spectrometer. The PDE was spin-coated onto a polished nickel substrate and detached after crosslinking for the analysis of the thin film.

The ^{1}H NMR measurements were recorded on a Varian XL-300 NMR spectrometer working at 300.032 MHz. The sample was dissolved in $CDCl_3$ in a 10-mm NMR tube at room temperature. The sample concentration was about 1% by weight for ^{1}H NMR. A proton-decoupled ^{13}C NMR spectrum was obtained with a Varian XL-300 NMR spectrometer working at 75.452 MHz. The sample concentration in a 10-mm tube was 10% by weight in $CDCl_3$.

The adhesion testing was conducted with an Elcometer 110 P.A.T.T.I. pneumatic tester according to ASTM Standard D 4541-95e1. The coating area to be tested was photodefined to a

circular shape (12.7 mm in diameter) matching the stud of the tester. The surfaces were gently roughened with sandpaper and adhered to the stud with a polyurethane adhesive. The accuracy of the adhesion strength was about 1%. The fracture surfaces were examined with an Olympus BX60 optical microscope equipped with a digital camera.

Models

In the literature, various approaches are presented that enable the evaluation of the solid surface free energy with measured contact angles by liquids with known surface tension.[21–28,34–50] All the models derived from these approaches are based on Young's equation (eq 1), and according to the model used, the measurement of one, two, three, or more probing liquid contact angles on the solid are needed:

$$\gamma_{lv} \cos\theta = \gamma_{sv} - \gamma_{sl} \quad (1)$$

In this case, the known parameters in Young's equation are γ_{lv} and θ, and it is expected that the solid–vapor surface free energy (γ_{sv}) can be provided by this equation. However, the solid–liquid surface free energy (γ_{sl}) is unknown. If this parameter could be expressed by another equation in terms of γ_{lv} and γ_{sv}, the problem could be solved.

Three basic approaches have been taken to solve this problem. The first approach aims to find a mathematical relationship for γ_{sl} in terms of γ_{lv} and γ_{sv} and then evaluate the unknown γ_{sv}. This approach has led to the formulation of several equation-of-state models, of which the latest modification has been presented very recently.[36] The second approach approximates the surface free energy of a solid with the concept of a critical contact angle.[28] The models based on this approach assume that the surface tension of a liquid that exhibits a zero contact angle on the solid surface equals γ_{sv}. However, these models generally yield values lower than those of the models based on the other approaches and require the use of many homologous probing liquids for the determination of γ_{sv}, which is time-consuming.[43] Because of these drawbacks, the second group of models is not considered further in this study. The approaches belonging to the third group were originally developed to provide an explanation of the results obtained within the context of the critical surface angle described previously.[28] These approaches divide the surface free energy into different components.[37,38] γ_{sl} is then expressed in terms of the components of γ_{lv} and γ_{sv}. Models formulated according to this approach include the geometric mean,[39,40] harmonic mean,[43] and acid–base[44–50] models, and the determination of γ_{sv} with these models requires the measurement of contact angles of two to three liquids on a given solid with known components of the surface tension.

Equation-of-State Model

If the values of γ_{lv}, γ_{sv}, and γ_{sl} are constant during an experiment and $\gamma_{lv} \cos\theta$ depends only on γ_{lv} and γ_{sv}, a mathematical relationship from such experimental contact-angle patterns should be deducible:

$$\gamma_{lv} \cos\theta = f(\gamma_{lv}, \gamma_{sv}) \quad (2)$$

The combination of eq 2 with Young's equation (eq 1) leads to the equation-of-state relationship:

$$\gamma_{sl} = f(\gamma_{lv}, \gamma_{sv}) \quad (3)$$

On the basis of Berthelot's rule, Li and Neumann[25] introduced a modified combining rule:

$$\varepsilon_{ij} = \sqrt{\varepsilon_{ii}\varepsilon_{jj}}\, e^{-\beta(\varepsilon_{ii} - \varepsilon_{jj})^2} \quad (4)$$

where ϵ_{ij} is the energy parameter of the interaction between dissimilar particles, ϵ_{ii} and ϵ_{jj} are the energy parameters between similar particles, β is an empirical parameter, and the square of $\epsilon_{ii} - \epsilon_{jj}$ is used for taking into account the symmetry of the combining rule. Because the energy of adhesion (W) is proportional to the energy parameter, eq 4 can be written as follows:

$$W_{sl} = \sqrt{W_{ss}W_{ll}}\, e^{-\beta(W_{ll} - W_{ss})^2} \quad (5)$$

Thermodynamically, the relation of the energy of adhesion per unit area of a solid–liquid pair is equal to the work required to separate the unit area of the solid–liquid interface:

$$W_{sl} = \gamma_{lv} + \gamma_{sv} - \gamma_{sl} \quad (6)$$

With the definitions $W_{ll} = 2\gamma_{lv}$ and $W_{ss} = 2\gamma_{sv}$ and a combination of eqs 5 and 6, the equation-of-state can be written as follows:

$$\gamma_{sl} = \gamma_{lv} + \gamma_{sv} - 2\sqrt{\gamma_{lv}\gamma_{sv}}\, e^{-\beta(\gamma_{lv} - \gamma_{sv})^2} \quad (7)$$

Combining eq 7 with Young's equation (eq 1) gives

$$\cos\theta = -1 + 2\sqrt{\frac{\gamma_{sv}}{\gamma_{lv}}}\, e^{-\beta(\gamma_{lv} - \gamma_{sv})^2} \quad (8)$$

The surface free energy (γ_{sv}) obtained from the model depends on the experimental constant β. γ_{sv} and β can be determined by a least-squares analysis technique from the set of γ_{lv} and θ data obtained with different liquids on the same solid. Spelt and Li[26] determined the value of β to be 0.0001247 $(m^2/mJ)^2$ from the data of measured contact angles with various liquids on three different surfaces. Recently, measurements with various liquids and polymer surfaces have yielded β values close to this value; this has resulted in a minor difference of approximately 0.1 mJ/m^2 when γ_{sv} is calculated.[36] Consequently, it seems that γ_{sv} could be evaluated by the equation-of-state model (eq 8) for a polymer surface when γ_{lv} and θ are known.

The model, however, contains some elements that cannot be regarded as correct. It basically attempts to prove that all liquids having the same surface tension will have the same contact angle on a given solid. In other words, the interfacial tension between any two phases having the same surface tension will always be the same. Several experimental as well as theoretical investigations have been carried out to test the proposed equation-of-state model, but the model has failed to meet the tests.[51,52]

Surface Free Energy Component Models

Fowkes[37,38] adopted a different approach by assuming that the attractive forces between the surface layers and liquid phase across the interface were independent of each other and additive and contributed to the surface free energy. Fowkes defined the dispersion force interaction between the solid and liquid phases and formulated their contribution to the surface free energy:

$$\gamma_{lv}(1 + \cos\theta) = 2(\gamma_s^d \gamma_{lv}^d)^{1/2} \quad (9)$$

This enabled the evaluation of the dispersion component (γ_s^d) of the surface free energy with liquids for which only dispersion forces operate like hydrocarbon liquids, but not the total γ_s.

Owens and Wendt[39] and Kaelble and Uy[40] extended Fowkes' equation to a geometric mean model that enabled the resolving of dispersion (γ_s^d) and polar (γ_s^p) components of the surface free energy:

$$\gamma_{lv_i}(1 + \cos\theta) = 2(\gamma_s^d \gamma_{lv_i}^d)^{1/2} + 2(\gamma_s^p \gamma_{lv_i}^p)^{1/2} \quad (10)$$

γ_s^d refers to dispersion (nonpolar) forces, and γ_s^p is assumed to refer to all polar (nondispersion) forces between the solid and liquid phases, including dipole–dipole, dipole-induced dipole, and hydrogen-bonding forces. The surface free energy is assumed to be a sum of γ_s^d and γ_s^p components, and so eq 10 provides a model for evaluating γ_s of solids with two liquids, one polar and one apolar, with known surface tension components (γ_{lv}^d and γ_{lv}^p). Because γ_s^d and γ_s^p are sensitive to surface chemistry, it was also proposed that the model could be used as a qualitative measure of the chemical composition of a surface. It should be noted that eq 10 also contains some questionable assumptions. It is not obvious that polar terms in eq 10 can be combined in Bertelot-type relations, which were originally developed for dispersion interactions between two different gas molecules. Another question is whether the solid surface tension is simply the sum of the interactive terms. One should be aware that van der Waals interactions among groups of molecules are not simply a sum of the individual pairwise interactions because they are affected by the presence of other interacting bodies in the vicinity.[53] The same assumption is also included in the following approach of Wu.[43]

Wu[43] also assumed interfacial forces to be additive and proposed a harmonic mean model based on empirical observations:

$$\gamma_{lv_i}(1 + \cos\theta) = \frac{4\gamma_s^d \gamma_{lv_i}^d}{\gamma_s^d + \gamma_{lv_i}^d} + \frac{4\gamma_s^p \gamma_{lv_i}^p}{\gamma_s^p + \gamma_{lv_i}^p} \quad (11)$$

Wu claimed that this model predicted the surface free energy components accurately in polar–polar systems.[43]

Continuing the work of Fowkes[37,38] and Owens and Wendt,[39] van Oss et al.[41,42] proposed the three-liquid acid–base model. It had been noticed that not all the interactions could be explained by simple division into dispersion and polar components, and the acid–base attraction between materials was expected to explain such cases.[42] In this model, γ_s is assumed to be the sum of a

Lifshitz/van der Waals component γ^{LW} (corresponding to γ^d) and a Lewis-acid–base component γ^{AB} (corresponding to γ^p):

$$\gamma_s = \gamma^{LW} + \gamma^{AB} \quad (12)$$

γ^{AB} results from electron–acceptor (γ^+) and electron–donor (γ^-) Lewis-acid–base interactions. The γ^{AB} term is expressed as a product of the electron–donor and electron–acceptor parameters, as they are not assumed to be additive:

$$\gamma^{AB} = 2\sqrt{\gamma^+\gamma^-} \quad (13)$$

Finally, the model was formulated by van Oss et al.:[41]

$$\gamma_{lv_i}(1 + \cos\theta) = 2[(\gamma_s^{LW}\gamma_{lv_i}^{LW})^{1/2} + (\gamma_s^+\gamma_{lv_i}^-)^{1/2} + (\gamma_s^-\gamma_{lv_i}^+)^{1/2}] \quad (14)$$

γ_s can be evaluated by eq 14 being solved simultaneously for three liquids (one apolar and two polar) used in the measurement of the contact angle with known surface tension components. In addition, a material is considered bipolar if both its γ^+ and γ^- components are greater than 0 ($\gamma^{AB} \neq 0$). A monopolar material has either an acidic or base nature; that is, either $\gamma^+ = 0$ and $\gamma^- > 0$ or $\gamma^- = 0$ and $\gamma^+ > 0$. An apolar material is neither an acid ($\gamma^+ = 0$) nor a base ($\gamma^- = 0$).

The surface free energy of a given solid is by no means a simple matter. It cannot be assumed to be a material constant because it is crucially dependent on the history of the sample, the surface reconstruction, the cleavage plane, and so forth. Therefore, it is our opinion that the surface free energy values of solids should be taken as indicative and not as explicit properties and only to give some indication about the property of the particular solid surface in question with a known history.

RESULTS AND DISCUSSION

Preparation of the Coatings

Centrifugal force can cause significant molecular chain orientation during spin coating, and so the surface free energy may appear anisotropic. However, no significant orientation was encountered with the epoxy coatings because the contact angles did not vary systematically (i.e., the samples gradually were rotated 90° while the eight repeated small drops of a given probing liquid were measured). The isotropy can be explained by the tendency of the polymer chains to twist back to their lower energy configurations if there are no constraints that prevent this. In this case, after the spin coating, the external force (i.e., centrifugal force) is absent. Also, kinetic constraints and so forth can be considered negligible (i.e., a diluted polymer at an elevated temperature during the solvent evaporation step) before the crosslinking takes place and freezes the structure.

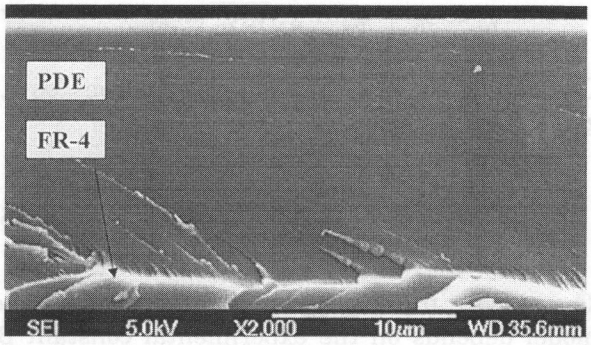

Figure 1. Cross-sectional fracture surface of the PDE coating on the FR-4 substrate.

The thickness of the coating was approximately 15 μm, as shown in Figure 1. This thickness is expected to be enough to provide a smooth surface for the contact-angle measurements. In fact, an AFM inspection showed that the average roughness of the untreated PDE surface was 0.3 nm. The roughness of the treated surfaces was measured to be 1.0 nm (chemical treatment) and 2.0 nm (RIE treatment). A surface roughness of 500 nm is reported to be the limit for having a significant influence on the contact angles measured by the sessile drop method.[35] Therefore, the surfaces can be considered smooth enough for reliable measurements. The measured contact angles are given in Table 2. Although the surfaces are considered smooth, slight surface heterogeneity is probable. This is because of the polymerization catalyst that can be added to PDE (up to 5 wt % of the prepolymer content), and it may affect the surface properties slightly.

Evaluation of the Models Used for Determining the Surface Free Energy

The need for the determination of the epoxy surface free energy became important when severe problems in preparing multilayer structures ap-

Table 2. Contact Angles (°) between the Probing Liquids and the Polymers[a]

	H_2O	DIM	FA	GL	1-Br	EG	DEG	DEC	TET
PDE	78.9	32.3	56.2	66.9	12.6	53.2	40.4	< 10	< 10
SD	2.8	1.7	3.1	2.1	1.0	2.4	2.2		
PTFE	109.8	nm	nm	99.1	76.4	nm	nm	32.0	40.3
SD	3.6			5.2	4.9			4.2	2.8

[a] nm = not measured for the material; SD = standard deviation.

peared with the unfilled PDE. The unfilled PDE was evaluated as a candidate for replacing the filled PDEs that had been used previously in integrated module boards.[30] Epoxies could be coated on filled PDEs even without surface treatment, whereas the unfilled PDE surface caused repulsion of the newly applied coating solution and the formation of islands instead of uniform coating. Furthermore, knowledge of the surface properties is essential if one is to ensure reliable adhesion between sequential layers. Although there is no direct correlation between surface free energy and adhesion strength, poor wettability can cause the formation of voids at the interface, thereby reducing adhesion strength.

Equation-of-State Model

The measured contact angles for the PDE were fitted in the equation-of-state curve. The equation-of-state model assumes the consistency of the surface free energy ($\gamma_{s,E}$) from one probing liquid to another and the dependence of $\gamma_{lv} \cos \theta$ on only γ_{lv}. Therefore, those contact-angle values scattering clearly from the curve were discarded. It is proposed that the halogen-containing probing liquids may involve reactions with the functional groups appearing on the PDE surface because the experimental contact angles for DIM and 1-Br were smaller than one could expect according to the aforementioned assumptions. However, the experimental contact angle for EG was higher than that assumed to result from swelling of the PDE surface. The accepted contact angles and respective liquid surface tensions (γ_{lv}) were employed in the determination of β and $\gamma_{s,E}$ with a least-squares analysis technique. The value for the surface free energy ($\gamma_{s,E}$) of the PDE was determined to be 36.6 mJ/m^2, and β equaled 0.0001193 (m^2/mJ)^2, as shown in Figure 2 along with the values of the employed liquids. The value of the empirical constant β differs only slightly from the value determined by Spelt and Li[26] [0.0001247 (m^2/mJ)^2]. If this value is used to determine the $\gamma_{s,E}$ value instead of the one determined here, the difference is only 0.1 mJ/m^2. $\gamma_{s,E}$ for the PTFE reference material was calculated by eq 5 with the value of 0.0001247 (m^2/mJ)^2 for β and the measured contact angles for H_2O, GL, and TET, resulting in 17.2, 18.5, and 20.9 mJ/m^2, respectively. The determined surface free energies agree well with the reported values determined by an equation-of-state model.[36] Nevertheless, the $\gamma_{s,E}$ values are clearly lower than the ones determined by the surface free energy component models in this study. It is to be noted that if the contact angles measured for DIM and 1-Br are used together with β [0.0001247 (m^2/mJ)^2] to calculate $\gamma_{s,E}$, the resulting value is comparable to the values determined by the surface free energy component models. In addition, the equation-of-state model does not give any information on the nature of the surface, such as the polarity or

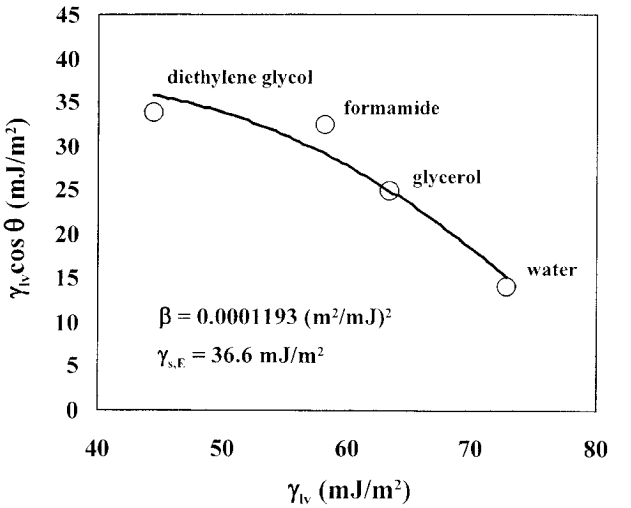

Figure 2. Plot of $\gamma_{lv} \cos \theta$ versus γ_{lv} for the PDE surface. The curve is the best fit of eq 8 to the experimental data of γ_{lv} and θ determined by a least-squares analysis technique.

Table 3. Surface Free Energies (mJ/m^2) of the Polymers as Determined by the HM Model

	Liquid Pair	$\gamma_{s,HM}$	γ_d	γ_p
PDE	DIM–H_2O	48.1	38.9	9.1
	DIM–GL	43.7	40.7	3.0
	DIM–FA	43.7	40.7	3.0
	DIM–EG	43.6	41.0	2.6
	DIM–DEG	43.5	41.8	1.7
PTFE	1-Br–H_2O	21.2	19.4	1.9

Table 5. Surface Free Energies (mJ/m^2) of the Polymers as Determined by the LW Model

	Liquid Combination	$\gamma_{s,LW}$	γ_s^{LW}	γ_s^{AB}	γ_s^-	γ_s^+
PDE	DIM–H_2O–GL	44.3	43.2	1.0	5.3	0.1
	DIM–H_2O–FA	43.5	43.2	0.3	6.1	~0
	1-Br–H_2O–GL	44.4	43.3	1.0	5.3	0.1
	1-Br–H_2O–FA	43.6	43.3	0.2	6.1	~0
PTFE	1-Br–H_2O–GL	17.2	16.9	0.1	0.6	~0

acidity, but only the evaluation of the total surface free energy. However, at the same time, the $\gamma_{s,E}$ value is obtained quite feasibly by the measurement of only one appropriately chosen probing liquid contact angle if the value of the constant β is adopted from the literature,[26] whereas the other models compared herein require the use of more liquids to obtain reliable surface information. However, because of the flaws associated with the model, as pointed out earlier, and because the model does not give any indication of the nature of the surface as already stated, the equation-of-state model was not used during the follow-up of the treated surfaces.

Surface Free Energy Component Models

The surface free energy component models used here are two-liquid geometric mean (GM),[39,40] two-liquid harmonic mean (HM),[43] and three-liquid acid–base (LW) models [44–50] that all assume intermolecular forces to be additive.[38,54] Tables 3–5 present the calculated surface free energy component values for the polymers with liquid pairs including apolar and polar liquid(s). The HM model gives higher surface free energy values and relative polarities ($x_p = \gamma^p/\gamma_s$) than the GM model. Similar behavior has been noticed previously with other polymers.[17,20] The LW model gives the highest γ_s values but the lowest polarities for the PDE. Slight scattering in the surface free energy values within the HM and GM models can be noticed, whereas the LW model gives remarkably consistent values for the PDE. In addition, the results from the LW model show that the polarity is quite low and that the PDE has a monopolar Lewis-base surface[55,56] because the γ^+ component is negligible. These results are in agreement with the reported values for epoxies.[57]

Table 4. Surface Free Energies (mJ/m^2) of the Polymers as Determined by the GM Model

	Liquid Pair	$\gamma_{s,GM}$	γ_d	γ_p
PDE	DIM–H_2O	43.6	39.7	3.8
	DIM–GL	43.6	42.9	0.7
	DIM–FA	44.4	43.4	1.0
	DIM–EG	43.7	43.2	0.5
	DIM–DEG	44.1	43.8	0.3
PTFE	1-Br–H_2O	21.2	21.0	0.1

It is to be noted that the carefully selected high-surface-tension ($\gamma_{lv} > \gamma_s$) liquid pairs including an apolar liquid (e.g., DIM or 1-Br) and polar liquid(s) (e.g., H_2O, GL, FA, EG, or DEG) give comparable γ_s, γ_s^d, and γ_s^p results for the PDE. Random combinations of the liquids result in extreme scattering of the components, as reported for other polymers as well.[17] Finally, it is shown that all the surface free energy component models give consistent results for the PDE. As a result, the obtained surface free energy components can be used as the reference values for the treated surfaces while the changes in their wettability properties are studied. The surface polarity is expected to increase with the surface treatments. The GM model gives comparable and reasonably consistent polarities when calculated from properly measured contact angles, yet it is a relatively easy and fast way to determine the surface free energy components. The HM model was omitted from the follow-up because of the lack of theoretical justifications. As Wu[43] himself pointed out, the model was based on empirical observations. The LW model gives surface free energy values comparable to those of the GM model. The only additional information that the LW model can give is the acid–base nature of the surface. In most cases, the model predicts that the surface of a solid is totally basic, even though an acidic nature would be expected.[58] Consequently, the GM model was selected for the follow-up of the treated surfaces with H_2O and DIM as the probing liquids.

Table 6. H_2O and DIM Contact Angles (°) on the 0-, 5-, 10; 15-, and 20-min-Treated PDE Surfaces[a]

			0	5	10	15	20
PDE (chemical)	H_2O		78.9	81.0	69.7	68.5	67.6
		SD	2.8	1.6	2.3	1.8	2.1
	DIM		32.3	29.9	30.6	28.0	28.4
		SD	1.7	1.7	0.4	2.0	1.4
PDE (RIE)	H_2O		78.9	73.8	63.5	63.1	64.5
		SD	2.8	2.1	3.6	2.6	4.0
	DIM		32.3	49.4	52.2	54.1	58.8
		SD	1.7	2.8	2.0	1.3	3.6

[a] SD = standard deviation.

Discussion of the Untreated Coating Surface

The structural factors that affect the physical properties of a polymer surface include the molecular weight, the composition of the polymer backbone, the functionality and its amount, the orientation of the chains, the crystallinity, the polarity, and the degree of crosslinking. It was shown by the contact-angle measurements on gradually rotated surfaces that there was no significant molecular chain orientation. The crystallinity of thermosetting polymers is low and, therefore, was not studied. The backbone of the epoxy is a glycidyl ether derivative of bisphenol A novolac. Backbone and functional groups arising from it, in particular, dictate the effects of the factors that are left: the nature and amount of functionality, the polarity, and the degree of crosslinking. These parameters are interrelated.

As the crosslinking proceeds, the functional groups are reformed, and the polarity of the surface is dictated mainly by the new functional groups or lack thereof. The covalent crosslinks of the PDE are expected to form in the Lewis-acid-catalyzed cationic ring-opening polymerization of the epoxy groups into the ether links. The chemical structure[59] (idealized) of the eight-functional PDE prepolymer does not contain hydroxyl groups or phenols. The lack of hydroxyl groups was shown by NMR because there was no chemical shift for a hydroxymethylene[60] (around δ = 62 ppm) in the ^{13}C NMR spectrum run on the PDE prepolymer; instead, the chemical shift for phenol[61] was detected at δ = 154.4 ppm. The FTIR analysis for the crosslinked sample showed a strong absorption peak at 3600 cm^{-1}, which is thought to originate from the phenol groups because no hydroxyl groups were found in the structure of the prepolymer.

The presence of phenol groups in the FTIR spectrum after the crosslinking means that the phenol groups are not reformed to a great extent during the crosslinking of the PDE. Therefore, the epoxies are the only functional groups of the polymer backbone taking part in the crosslinking reaction. Because of this, the hydrophobic nature of the PDE surface should increase as the degree of crosslinking increases because the polar epoxy groups are reformed into less polar ether links. This was verified experimentally as the contact angle of H_2O on the slightly crosslinked surface (baked at 90 °C for 30 min) gradually increased from 73 to 80° on the fully crosslinked PDE (baked at 160 °C for 2 h).

The increase in the hydrophobic nature of the surface and the findings from FTIR and NMR are consistent with the provided crosslinking mechanism. The polarity of the crosslinked epoxy, as determined by the surface free energy component models, was very low. This also agrees well with the findings about the structure of the prepolymer and the crosslinking mechanism. The surface free energy evaluated with the different models for the PDE agreed well with the reported[57] value for crosslinked epoxy. In conclusion, adhesion-related problems are more than expectable because the coating surface appears relatively smooth, hydrophobic, low in polarity, and chemically highly inert after crosslinking.

Evaluation of the Treated Surfaces

Table 6 presents the contact angles between the probing liquids (H_2O and DIM) and the treated PDE in comparison with the untreated surface. The chemical and RIE treatments produced the desired effect on the PDE surface as the H_2O

contact angle was reduced as a function of the treatment time. The reduction of the contact angle is most likely the result of the formation of polar (oxygen containing) groups on the polymer surface.[33] In contrast to the measurements with H_2O, the DIM contact angles were increased by the RIE treatment, and this suggests that the total surface free energy is not increased by the treatment. The wettability of the PDE surfaces was tested also with the PDE solution. A small improvement in the wettability of the PDE surface was detected, as can be seen from the contact-angle results for the untreated (24°), chemically treated (22°), and RIE-treated (17°) surfaces. These surfaces were treated for 15 min. The surface free energies ($\gamma_{s,GM}$) calculated with the GM model are 47.2 mJ/m^2 (x_p = 17.6%) and 41.5 mJ/m^2 (x_p = 42.9%) by the chemical and RIE treatments, respectively. A more detailed development of the polarity and surface free energy as a function of the treatment time is given in Table 7. Even though the surface free energy (by the GM model) did not increase much and actually decreased with the RIE treatment, the polarity was clearly increased by both the chemical and RIE methods.

Adhesion Results

Adhesion at the FR-4/PDE interface appears good because of the seemingly rough surface of the underlying material (see Fig. 3). Roughness enables mechanical interlocking after the crosslinking of the PDE has taken place inside the microcavities, forming microanchors. This leads to cohesive fracture at the FR-4/PDE interface (see Fig. 1). Nevertheless, the surfaces of the built-up layers of the PDE lack sufficient roughness for the mechanical interlocking unless the surfaces are intentionally roughened. As shown for the PDE, the roughness of the treated surfaces was only a fraction of the FR-4's roughness. Therefore, the lack of improvement in the adhesion strength at the interface between the treated PDE and the sequential PDE is reasonable because mechanical interlocking is not possible. Also, the change in the surface chemistry of the treated surfaces does not contribute noticeably to the adhesion through improved wettability. However, a distinct improvement in the adhesion strength is obtained if the underlying PDE is not fully crosslinked before the application of the PDE sequential coating (see Fig. 4). The photodefining properties are achieved already in the softer bake stage (90 °C for 30 min), and further crosslinking is not necessary from the point of view of the build-up process. In addition, the residual reactivity, that is, the unreacted epoxy groups, on the PDE surface react with the sequential PDE layer during its crosslinking bake. This, in turn, leads to good adhesion between the PDE layers and cohesive fracture at the PDE/FR-4 interface.

Table 7. Surface Free Energies (mJ/m^2) and Polarities (%) of the 0-, 5-, 10, 15-, and 20-min-Treated PDEs as Determined by the GM Model with H_2O and DIM as the Probing Liquids

PDE		$\gamma_{s,GM}$	γ^d_s	γ^p_s	x_p
Untreated		43.6	39.7	3.8	8.7
Chemical	5	44.3	41.5	2.8	6.3
	10	46.1	38.1	8.0	17.4
	15	47.2	38.9	8.3	17.6
	20	47.4	38.5	8.9	18.8
RIE	5	37.9	28.8	9.1	24.0
	10	41.8	24.9	16.9	40.4
	15	41.5	23.7	17.8	42.9
	20	39.5	21.2	18.3	46.3

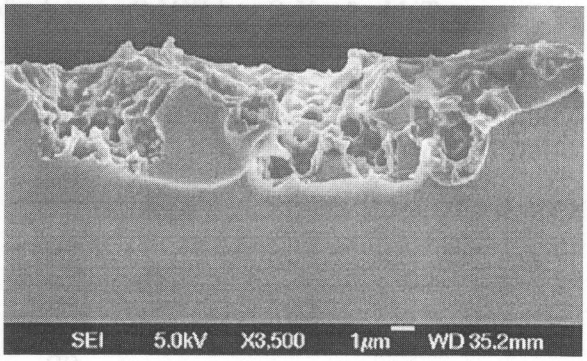

Figure 3. Cross-sectional fracture surface of FR-4 showing its seemingly rough horizontal surface.

The adhesion at the PDE/PDE interface is improved. Nevertheless, it is known that for good adhesion to be achieved between the PDE and electrolessly deposited copper, a seemingly rough surface is demanded. Therefore, alternative means to improve the adhesion have to be considered in the future if the unfilled PDE is to be implemented in the multilayer PWB fabrication as an interlayer. Approaches to improve the adhesion between the sequential copper and PDE layers include the utilization of vacuum technologies (e.g., sputter deposition of a Cr adhesion-promoting layer before Cu metalization) and the

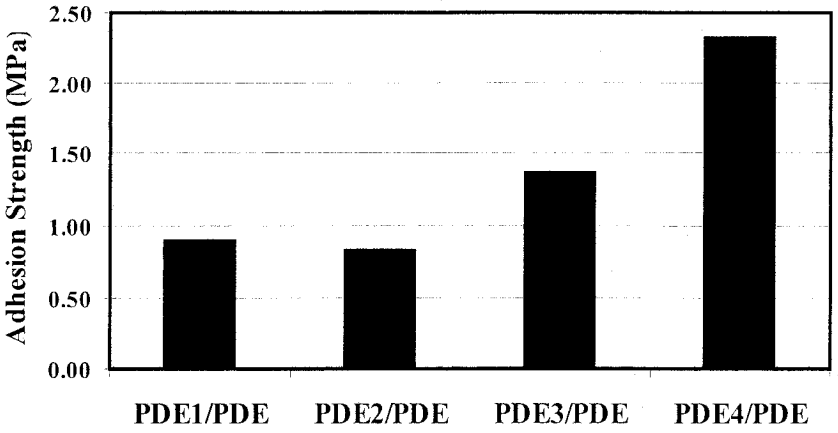

Figure 4. Adhesion strength between the PDE coating and untreated (PDE1), chemically treated (PDE2), RIE-treated (PDE3), and less crosslinked (PDE4) underlying PDE.

application of coupling agents to the metalization before the PDE coating. However, there exist also many applications that allow the use of surface roughening before metalization. Therefore, the blending of a chemically weak phase into the PDE, to act as a sacrificial phase during the chemical etching and, therefore, provide surface roughness, can lead to success in several applications.

CONCLUSIONS

The solid surface free energy (γ_s) of the PDE was evaluated to be 43.6 mJ/m^2 from the advancing contact angles measured by the sessile drop method with a geometric mean model. The equation-of-state and three surface free energy component models were evaluated, and their limitations and advantages were discussed. The equation-of-state model resulted in a lower value of the surface free energy than the other models. The surface free energy component models resulted in consistent values with properly selected liquid combinations. The γ_s value for the PDE agreed with the values reported in the literature for epoxy.[57] In addition, the coating surface appears isotropic with respect to the surface free energy. Also, the low polarity that is found for the crosslinked PDE is reasonable in view of its chemical structure. The chemical treatment increased γ_s somewhat, but with RIE, γ_s decreased from the original level. However, the polarity of the PDE surface (9%) increased more with RIE (43%) than with the chemical treatment (18%). The wettability of the crosslinked PDE coating improved slightly after the treatments, as tested by the PDE solution. However, the adhesion strength of the PDE coating to the underlying PDE was not noticeably affected by the treatments, but it was clearly improved when applied to the PDE surface, which exhibited residual reactivity; that is, the underlying PDE was intentionally less crosslinked and, therefore, contained epoxy groups capable of reacting with the sequential PDE coating. The average roughness of the untreated PDE was 0.3 nm and increased to 1.0 and 2.0 nm after the chemical and RIE treatments, respectively. This level of roughness cannot contribute noticeably to the adhesion from a mechanical interlocking point of view.

The authors acknowledge Ms. Laura Orre from Ashland Finland Oy for her contribution to the contact-angle measurements and Mr. Kimmo Henttinen from VTT Microelectronics for the AFM measurements and Mr. Andrei Olykainen for technical assistance in the sample preparation. This work was financially supported by the Academy of Finland.

REFERENCES AND NOTES

1. Kelley, E. J.; Gonzalez, C. G.; Roesch, M.; Ehrler, S.; Holden, H.; Nakahara, H. In Printed Circuits Handbook, 5th ed.; Coombs, C. F., Jr., Ed.; McGraw-Hill: New York, 2001; Part 2, pp 5.3–12.21; Part 4, pp 21.3–23.15.
2. Gonzalez, C. G. Board Authority 2000, 3, 54–62.
3. Akahoshi, H.; Kawamoto, M.; Itabashi, T.; Miura, O.; Takahashi, A.; Kobayashi, S.; Miyazaki, M.;

Mutoh, T.; Wajima, M.; Ishimaru, T. IEEE Trans Components Packaging Manufacturing Technol Part A 1995, 18, 127–135.
4. Kujala, A.; Kivilahti, J. K. Proc. 35th IMAPS Nordic Annual Conference, Stockholm, Sweden, Sept. 1998, pp 269–273.
5. Holden, H. Circuit World 1997, 23, 14–17.
6. Zhang, S.; De Baets, J.; Van Calster, A. Microelectron Reliability 1999, 39, 1337–1341.
7. Takeuchi, M.; Yoshida, K.; Iida, A.; Ohdaira, H. Proc. 6th IEEE/CHMT International Electronic Manufacturing Technology Symposium, Nara, Japan, April 1989, pp 136–140.
8. Kujala, A.; Tuominen, R.; Kivilahti, J. K. Proc. 49th IEEE Electronic Components and Technology Conference, San Diego, CA, June 1999, pp 155–159.
9. Li, W.; Tummala, R. Proc. 48th IEEE Electronic Components and Technology Conference, Seattle, WA, May 1998, pp 151–157.
10. Neugurger, D.; Jacobus, D.; Lenihan, T.; Robinson, C.; Matijasevic, G.; Ha, L.; Gallagher, C.; Castello, C.; Gandhi, P. Proc. 7th IEEE International Conference on Multichip Modules and High Density Packaging, Denver, CO, April 1998, pp 218–223.
11. Ge, J.; Kivilahti, J. K. J Adhes Sci Technol 2001, 15, 1133–1143.
12. Good, R. J. In Adhesion Science and Technology, Polymer Science and Technology; Lee, L. H., Ed.; Plenum: New York, 1975; Vol. 9A, pp 107–127.
13. Mittal, K. L. In Adhesion Science and Technology, Polymer Science and Technology; Lee, L. H., Ed.; Plenum: New York, 1975; Vol. 9A, pp 129–171.
14. Neumann, A. W.; Good, R. J. In Techniques of Measuring Contact Angles, Surface and Colloid Science; Good, R. J.; Stromberg, R. R., Eds.; Plenum: New York, 1979; Vol. 11.
15. Kwok, D. Y.; Gietzelt, T.; Grundke, K.; Jacobasch, H. J.; Neumann, A. W. Langmuir 1997, 13, 2880–2894.
16. Kwok, D. Y.; Neumann, A. W. Colloids Surf A 2000, 161, 49–62.
17. Ma, K.; Chung, T. S.; Good, R. J. J Polym Sci Part B: Polym Phys 1998, 36, 2327–2337.
18. Augsburg, A.; Grundke, K.; Pöschel, K.; Jacobasch, H. J.; Neumann, A. W. Acta Polym 1998, 49, 417–426.
19. Balkenende, A. R.; van de Boogaard, H. J. A. P.; Scholten, M.; Willard, N. P. Langmuir 1998, 14, 5907–5912.
20. Ho, C. C.; Khew, M. C. Langmuir 2000, 16, 1407–1414.
21. Sharma, P. K.; Hanumantha Rao, K. Adv Colloid Interface Sci 2002, 98, 341–463.
22. Girifalco, L. A.; Good, R. J. J Phys Chem 1957, 61, 904–909.
23. Good, R. J.; Girifalco, L. A.; Kraus, G. J Phys Chem 1957, 62, 1418–1422.
24. Good, R. J.; Girifalco, L. A. J Phys Chem 1960, 64, 561–565.
25. Li, D.; Neumann, A. W. J Colloid Interface Sci 1990, 137, 304–307.
26. Spelt, J. K.; Li, D. In Applied Surface Thermodynamics; Neumann A. W.; Spelt, J. K., Eds.; Marcel Dekker: New York, 1996.
27. Good, R. J.; Kvikstad, J. A.; Balley, W. O. J Colloid Interface Sci 1971, 35, 314–327.
28. Fox, H. W.; Zisman, W. A. J. J Colloid Sci 1950, 5, 514–531.
29. Li, D.; Xie, M.; Neumann, A. W. Colloid Interface Sci 1993, 271, 573–580.
30. Tuominen, R.; Kivilahti, J. K. Proc. 4th International Conference on Adhesive Joining and Coating Technology in Electronics Manufacturing, Adhesives in Electronics 2000, Helsinki, Finland, June 2000, pp 269–273.
31. Ge, J.; Tuominen, R.; Kivilahti, J. K. Proc. 4th International Conference on Adhesive Joining and Coating Technology in Electronics Manufacturing, Adhesives in Electronics 2000, Helsinki, Finland, June 2000, pp 248–252.
32. van Heuven, J. H. C. IEEE Trans Microwave Theory Tech 1974, 22, 841–849.
33. Ge, J.; Kivilahti, J. K. J Appl Phys 92, in press.
34. van Oss, C. J. In Polymer Surfaces and Interfaces; Feast, W. J.; Munro, H. S.; Richards, R. W., Eds.; Wiley: Chichester, England, 1993; Vol. 2.
35. Wu, S. Polymer Interface and Adhesion; Marcel Dekker: New York, 1982.
36. Kwok, D. Y.; Neumann, A. W. Colloids Surf A 2000, 161, 31–48.
37. Fowkes, F. M. J Phys Chem 1963, 67, 2538–2543.
38. Fowkes, F. M. In Acid–Base Interactions; Mittal, K. L.; Anderson, V. R., Jr., Eds.; VPS: Utrecht, The Netherlands, 1991; pp 93–115.
39. Owens, D. K.; Wendt, R. C. J Appl Polym Sci 1969, 13, 1741–1747.
40. Kaelble, D. H.; Uy, K. C. J Adhes 1970, 2, 50–60.
41. van Oss, C. J.; Good, R. J.; Chaudhury, M. K. Langmuir 1988, 4, 884–891.
42. van Oss, C. J.; Good, R. J.; Chaudhury, M. K. J Colloid Interface Sci 1986, 111, 378–390.
43. Wu, S. J Polym Sci Part C: Polym Symp 1971, 34, 19–30.
44. van Oss, C. J.; Chaudhury, M. K.; Good, R. J. Chem Rev 1988, 88, 927–941.
45. van Oss, C. J.; Ju, L.; Chaudhury, M. K.; Good, R. J. J Colloid Interface Sci 1989, 128, 313–319.
46. van Oss, C. J.; Good, R. J. J Macromol Sci Chem 1989, 26, 1183–1203.
47. van Oss, C. J. J Dispersion Sci Technol 1990, 11, 491–502.
48. van Oss, C. J.; Arnold, K.; Good, R. J.; Gawrisch, K.; Ohki, S. J Macromol Sci Chem 1990, 27, 563–580.
49. van Oss, C. J.; Good, R. J.; Busscher, H. J. J Dispersion Sci Technol 1990, 11, 75–81.

50. van Oss, C. J.; Giese, R. F., Jr.; Good, R. J. Langmuir 1990, 6, 1711–1713.
51. Morrison, I. D. Langmuir 1991, 7, 1833–1836.
52. Johnson, R. E.; Dettre, R. H. Langmuir 1989, 5, 293–295.
53. Mayers, D. In Surfaces, Interfaces and Colloids: Principles and Applications; VCH: New York, 1991; p 433.
54. Fowkes, F. M.; McCarthy, D. C.; Mosfata, M. A. J Colloid Interface Sci 1980, 78, 200–206.
55. Costanzo, P. M.; Giese, R. F.; van Oss, C. J. In Acid–Base Interactions; Mittal, K. L.; Anderson, V. R., Jr., Eds.; VPS: Utrecht, The Netherlands, 1991; pp 135–143.
56. Good, R. J.; Srivatsa, N. R.; Islam, M.; Huang, H. T. L.; van Oss, C. J. In Acid–Base Interactions; Mittal, K. L.; Anderson, V. R., Jr., Eds.; VPS: Utrecht, The Netherlands, 1991; pp 79–89.
57. Berger, E. J. In Acid–Base Interactions; Mittal, K. L.; Anderson, V. R., Jr., Eds.; VPS: Utrecht, The Netherlands, 1991; pp 207–225.
58. Berg, J. In Wettability; Berg, J., Ed.; Surfactants Science Series 49; Marcel Dekker: New York, 1993; pp 75–148.
59. Shaw, J. M.; Gelorme, J. D.; LaBianca, N. C.; Conley, W. E.; Holmes, S. J. IBM J Res Dev 1997, 39, 81–96.
60. Turunen, M. P. K.; Korhonen, H.; Tuominen, J.; Seppälä, J. V. Polym Int 2002, 51, 92–100.
61. Park, B. D.; Riedl, B. J Appl Polym Sci 2000, 77, 1284–1293.